

Robust Control and Diagnostic Strategies for Xerographic Printing

Perry Y. Li
Department of Mechanical Engineering
University of Minnesota
111 Church St. SE,
Minneapolis, MN 55455

Abstract

In this paper, we outline two strategies for the maintainence and optimization of the printing quality of xerographic systems. The first strategy is concerned with the management of the effect of disturbances and system variations in the context of control of the tone reproduction curve via a robust control methodology. The second strategy deals with larger scale faults and capability degradation in the xerographic process. In this case, a Bayesian Network based diagnostics strategy is proposed to detect the fault state and the state of the capability of the printer. Based on these, the controller be can reconfigured so as to optimize the printer's performance under degraded mode.

1. Introduction

The most fundamental function of a digital xerographic print engine is to produce on the output media printed images that are as similar as possible to the desired input images. As such, printers can be thought of as transformations of desired input images to printed output images. The ideal for such a transformation is the unity transformation.

The transformation for an actual printer, is however, subject to many disturbances due to variation in operating conditions such as humidity, toner and photoreceptor age, and geometry etc., as well as more drastic changes of the system, such as system faults and component degradation. In a broad sense, the goal of xerographic control is to maintain this transformation from the desired image to the output image as close to unity as possible, despite these variations.

In this paper, we discuss two aspects of this control objective. The first is concerned with the robust stabilization of the *tone reproduction curve*, in the face of moderate system variation and disturbance. The second aspect is concerned with larger scale variations and system degradations. Faults in and degradations of the system components can reduce the feasible capability of the overall system (such as a reduction in the color gamut). Instead of merely shutting down the system when these faults occur, it might be advantageous if the machine can remain available, albeit at a degraded quality. In these cases, the faults and degree of component degradations need to be actively diagnosed and identified, so that the control scheme can be reconfigured to make the best use of the current capability of the system. Ability of the system to self-diagnose faults can also improve serviceability and help minimize servicing times.

1.1. The TRC Stabilization problem

A color printer / copier will attain good color rendering quality if the Image Output Terminal (IOT) can produce the desired tone for each of the four primary color separations (Cyan, Magenta, Yellow, Black) as requested. In a digital printer, the desired continuous tone image is first translated into one of many halftone patterns, each labelled by its *halftone density*, using a halftoning algorithm. Given the halftone image, the IOT then physically lays down the appropriate amount of toner on the output medium. The toner image should ideally approximate the desired continuous tone image. A Tone Reproduction Curve (TRC) of the IOT is a characterization of this latter physical process and determines the amount of toner that would be deposited on the output media when a halftone image of a certain half-tone density is given. Thus, the TRC is a mapping $\Phi : [0,1] \to \Re$, so that $\Phi(\mathtt{tone})$ represents the developed toner area coverage on the photoreceptor, when a halftone image of density $\mathtt{tone}$ is presented.

In xerography [4], the TRC is subject to uncontrolled operating conditions. Variation in these, such as temperature, humidity, toner age and charge density etc. can cause the TRC to vary so that the IOT can produce unpredictable output images at various times with the same input halftone image. Thus, maintaining the TRC constant, or the stabilization of the TRC, is necessary to avoid having to retune the half-toning algorithm, and to allow the same halftone image to be reused over time. Thus, the first control strategy involves the design of a TRC stabilizing controller so that the TRC remains close to the nominal curve despite variations in uncontrolled operating condi-

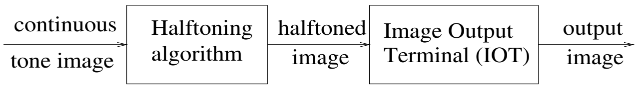

Figure 1: Image path in a digital printing system. The composition of the half toning and IOT should ideally be a unity transformation.

tions.

The TRC is a potentially infinite dimensional object (it is a function of $[0, 1]$). However, there are only a small number of actuators available for control (e.g. Scorotron grid voltage, laser power, development voltage). Current technology (such as the use of sensor patches and Toner area coverage (TAC) sensors) only allows the TRC to be sampled at a small number of tones. The entire TRC is not available for feedback. Typically, an IOT has m=3 actuators and samples the TRC at n=1 to 5 tones. Consequently, the control must take caution that the performance of the TRC does not degrade significant even at the un-measured tones. In this paper, we describe a robust controller for TRC stabilization that aims to ensure that the *entire* TRC is close to nominal despite disturbances and plant variation.

1.2. Xerographic diagnostics problem

The number of sensors available in a xerographic engine for monitoring the components' health is much smaller than the number of possible faults. Therefore, faults and the health states cannot be directly detected and must be inferred from observations. These observations may be produced from many sets of fault conditions. The diagnostic problem is to determine the set of fault states and / or component degradation that best explain the observations.

In this paper, we describe a probabilistic diagnostic approach based on Bayesian Belief Network (BBN). Probabilistic diagnostic approaches have the advantage over deterministic approaches in which causal relationships are encoded in crisp logic. In probabilistic approaches, the conditional probability of the failure when an evidence has been introduced can be used to indicate the confidence level of, and therefore to rank, the various diagnosis. In constrast, every logically consistent diagnosis has equal footing in a deterministic framework. An important issue associated with a rigorous implementation of probabilistic diagnostic system is that of computation and storage burden. It is because diagnostic inference involves computation of joint probabilities of the relevant system variables. BBN is an efficient implementation by avoiding the storage of the entire joint probability table. Instead, it uses the causal relationships between variables and stores the conditional probability relationships. BBN has been successfully applied in many disciplines including engineering decision support systems.

2. Robust TRC Stabilization

2.1. Problem Formulation

Assume that the TRC can be well represented by sampling at p (can be large) tones. The model of the IOT is of the following form:

$$\mathbf{e}(k) = \phi_d \cdot \mathbf{d}(k) + \hat{\phi} \cdot [\mathbf{I} + \Delta(k)\mathbf{W}_u] \cdot \mathbf{u}(k) \quad (1)$$

$$\mathbf{y}(k) = \mathbf{C} \cdot \mathbf{e}(k) \quad (2)$$

where $\mathbf{u}(k) \in \Re^m$, with $m << p$, is the vector of incremental actuator values from the nominal control (which would generate the nominal TRC in the absence of model uncertainty and disturbances), $\mathbf{e}(k) \in \Re^p$ is the TRC error which is the deviation of the printed toner area coverage from the nominal ones at the various tones, $\mathbf{y}(k) \in \Re^n$, $n << p$ are the samples of the TRC which can be used for feedback, $k = 0, 1, \ldots$ is the time index. In Eq.(1),

$$\hat{\phi} \cdot (\mathbf{I} + \Delta(k)\mathbf{W}_u) \in \Re^{p\times m} \quad (3)$$

is the sensitivity of the TRC to actuator settings in which $\hat{\phi} \in \Re^{p\times m}$ is the nominal sensitivity function, $\mathbf{d}(k) \in \Re^{n_d}$ are the disturbances, ϕ_d is the sensitivity of the TRC to disturbances. The actual sensitivity of the TRC to the actuator values in (3) consists of the *known* nominal part, $\hat{\phi} \in \Re^{p\times m}$; and the *unknown* uncertain part, $\hat{\phi}\Delta(k)\mathbf{W}_u \in \Re^{p\times m}$, where $\mathbf{W}_u \in \Re^{m\times m}$ is a matrix of given uncertainty weights and $\Delta(k) \in \Re^{m\times m}$ is a possibly time varying multiplicative uncertainty. By letting $\Delta(k) \in \Re^{m\times m}$ be undefined and arbitrary, Eq.(3) describes a family of printers which have different characteristics due to variabilities in manufacturing and operating conditions.

The nominal sensitivity $\hat{\phi}$ can be obtained by averaging the Jacobian linearizations about various operating points or by taking the least squares fit to a factorial experiment. The disturbances $\mathbf{d}$ and ϕ_d which is the sensitivity of the TRC to $\mathbf{d}$, can be defined to be quite general. For example, $\mathbf{d}(k) \in \Re^p$ can be arbitrary and which have effect on a local region on the TRC: Let $\phi_d(i, j)$, $1 \leq i \leq p$, $1 \leq j \leq n_d$ denote the i-th row, j-th column of ϕ_d, and let the disturbance sensitivity $\phi_d \in \Re^{p\times n_d}$ to be defined by:

$$\zeta(i, j) = \exp^{-\frac{(i-j)^2}{2\sigma^2}}, \;\; \phi_d(i, j) = \frac{\zeta(i, j)}{\sum_{k=1}^{p} \zeta(i, k)}. \quad (4)$$

where σ determines the width of the Gaussian functions.

If $\mathbf{U}(z) = \mathbf{K}(z)\mathbf{Y}(z)$, where $\mathbf{K}(z)$ is some linear feedback controller (z is the z-transform variable), then the closed loop system can be expressed as a Linear Fractional Transformation (LFT) as in Fig. 2 where $\mathbf{P}$ is a known matrix based on nominal knowledge of the system. In this setting, the general goal is to find a controller $\mathbf{K}(z)$ so that

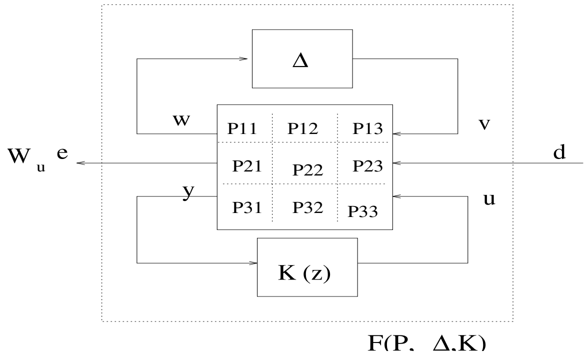

Figure 2: *LFT representation of linear system model*

under the "worst" case scenario for as large a class of uncertainty $\Delta(\cdot)$ as possible, the induced 2-norm from $\mathbf{d}(\cdot)$ to the weighted TRC error $\mathbf{W}_e\mathbf{e}(\cdot)$ is minimized. One constraint, however, is that the controller must be causal i.e. control action $\mathbf{u}(k)$ should only depend on past measurements $\mathbf{y}(k-1), \mathbf{y}(k-2), \mathbf{y}(k-3), \ldots,$.

2.2. Robust Static Performance

The controller design is much simplified by making use of the static nature of the xerographic process, and the fact that disturbances are generally slowly varying. In this case, the performance optimization objective can be restricted to the steady state and it becomes a convex problem. To wit, suppose that the disturbances $\mathbf{d}(k)$ is constant and that the controller $\mathbf{K}(z)$ is stabilizing. Thus, under steady state condition, $\mathbf{d}(k) = \mathbf{d}^\infty =$ constant, $\mathbf{u}(k) = \mathbf{u}^\infty =$ constant, $\mathbf{e}(k) = \mathbf{e}^\infty =$ constant, $\mathbf{y}(k) = \mathbf{y}^\infty =$ constant, $\mathbf{u}^\infty$ and $\mathbf{y}^\infty$ are related by the D.C. gain of the controller $\mathbf{K}^\infty = \mathbf{K}(z=1)$:

$$\mathbf{u}^\infty = \mathbf{K}^\infty \mathbf{y}^\infty.$$

Notice that in the steady state, $\Delta(k)$ in (1) is also a constant, Δ^∞ (although it may depend on $\mathbf{K}^\infty$). Since $\mathbf{W}_e\mathbf{e}^\infty$ is linear with respect to $\mathbf{d}^\infty$, there exists some matrix, $\mathbf{F}(\mathbf{P}, \boldsymbol{\Delta}^\infty, \mathbf{K}^\infty) \in \Re^{\mathbf{p}\times\mathbf{m}}$:

$$\mathbf{W}_e\mathbf{e}^\infty = \mathbf{F}(\mathbf{P}, \Delta^\infty, \mathbf{K}^\infty) \cdot \mathbf{d}^\infty.$$

The following steady state performance index will be optimized:

$$\bar{\gamma}(\mathbf{K}^\infty) = \min\left\{\gamma : \sup_{\|\Delta^\infty\| \leq \frac{1}{\gamma}} \bar{\sigma}\left(F(\mathbf{P}, \boldsymbol{\Delta}^\infty, \mathbf{K}^\infty)\right) \leq \gamma\right\} \tag{5}$$

where $\overline{\sigma}[\cdot]$ denotes the maximum singular value (induced 2 norm) of its argument. The optimal controller D.C. gain is

$$\mathbf{K}_{opt} := \operatorname*{argmin}_{\mathbf{K}^\infty} \bar{\gamma}(\mathbf{K}^\infty).$$

The performance index (5) is used instead of the more common index in which the bound on the size of $\|\Delta^\infty\|$ is specified because the size of the uncertainty is generally not easy to estimate. By minimizing the performance index in (5), we aim to simultaneously improve the worst case performance and increase the size of the uncertainty set $\|\Delta^\infty\|$. The weighting matrices $\mathbf{W}_u$ and $\mathbf{W}_e$ generate the frontiers of the tradeoff between robustness and performance. If $\bar{\gamma}_{opt} := \bar{\gamma}(\mathbf{K}_{opt})$, then for all uncertainties satisfying $\|\Delta^\infty\| \leq 1/\bar{\gamma}_{opt}$, the steady state TRC error $\mathbf{W}_e\mathbf{e}^\infty$ will be less than $\bar{\gamma}_{opt}\|\mathbf{d}^\infty\|_2$.

Notice that the response of the TRC at the measured tones conforming to the nominal, i.e. $\mathbf{y} = 0$, does not imply that $\|\mathbf{W}_e\mathbf{e}\|_2$ is minimized. It is because $\mathbf{y}$ can be made to vanish at the expense of TRC errors at the *unmeasured* tones.

2.3. Two-step Controller Design

Step 1: Finding $\mathbf{K}_{opt}$ Without going into details, the optimal D.C. gain $\mathbf{K}_{opt}$ can be found via the method of bisection using a result in [5]. For details, the readers are referred to [2]. In this procedure, we first find a lower and upper bound γ_l and γ_u so that $\gamma_l < \gamma_{opt} \leq \gamma_u$. Since the optimal solution is characterized by its satisfaction of a pair of Linear Matrix Inequalities (LMI), and the optimization problem is convex, the bounds are successively halved by checking the conditions until $\gamma_u - \gamma_l$ is within the desired accuracy. Finally, the optimal gain $\mathbf{K}_{opt}$ can be computed based on $\gamma = \gamma_u$ according to [5].

Step 2: Realizing $\mathbf{K}(z)$ The proportional controller $\mathbf{u}(k) = \mathbf{K}_{opt}\mathbf{y}(k)$ cannot be realized because $\mathbf{y}(k)$ is not available until $\mathbf{u}(k)$ is issued. A causal controller $\mathbf{K}(z)$ in which $\mathbf{u}(k)$ does not depend $\mathbf{y}(j \geq k)$ must now be defined with the property that the optimal D.C. gain $\mathbf{K}_{opt}$ is also achieved. Let a realization of the controller be of the form:

$$\mathbf{u}(k+1) = \mathbf{A}\,\mathbf{u}(k) + \mathbf{B}\,\mathbf{y}(k). \tag{6}$$

The controller will have the suboptimal D.C. gain if:

$$\mathbf{K}_{opt} = (\mathbf{I} - \mathbf{A})^{-1}\mathbf{B}.$$

The nominal closed loop system, i.e. when $\Delta(k) = 0$, will be stable if:

$$\left|\text{eig}\left(\mathbf{A} + \mathbf{BC}\hat{\phi}\right)\right| < 1.$$

Define $\mathbf{L}$ to be the nominal *loop gain*: $\mathbf{L} = \mathbf{K}_{opt}\mathbf{C} \cdot \hat{\phi}$, then, the two design conditions become:

$$|\text{eig}\left(\mathbf{L} + \mathbf{A}\,(\mathbf{I} - \mathbf{L})\right)| < 1 \tag{7}$$

$$\mathbf{B} = (\mathbf{I} - \mathbf{A})\mathbf{K}_{opt}. \tag{8}$$

If $\mathbf{I} - \mathbf{L}$ is non-singular, it can be shown [2] that the closed loop system matrix ($\mathbf{A}_c$ below) of the nominal system,

$$\mathbf{A}_c = \mathbf{L} - \mathbf{A}(\mathbf{I} - \mathbf{L}) = \mathbf{A} + \mathbf{BC}\hat{\phi} \tag{9}$$

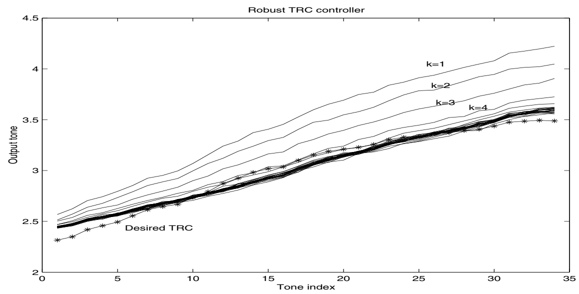

Figure 3: *Response of system using proposed robust controller with eigenvalues at* 0.8.

as well as the eigenvalues can be chosen arbitrarily. Hence, one can first choose a desirable stable closed loop matrix $\mathbf{A}_c$ and then solve for $\mathbf{A}$ and $\mathbf{B}$ from (8) and (9). At this point, the stability of closed loop system for the various uncertainty (possibly time varying) with $\|\Delta(k)\| \leq \delta$, can also be evaluated (see [2] for details).

2.4. Experimental Results

The proposed controller has been experimentally tested on a legacy digital xerographic Image Output Terminal (IOT). In this setup, the grid voltage of the charging system, the laser power in the exposure system and the bias voltage in the development system are available as xerographic actuators, and a single TAC sensor is available for sampling the TRC. In order to evaluate the controller performance, the entire TRC needs to be measured. This is achieved by producing an image of continuously increasing tone (a wedge) in the region of the photoreceptor which is ordinarily used for customer images. The wedge is printed under and is read by the TAC sensor. It is therefore possible to sample the TRC at as many tones as we desire. In our case, the TRC is judged to be adequately approximated by $p = 34$ uniform samples.

In our controller design, it was assumed that the disturbances are $\mathbf{d}(k) \in \Re^{n_d=34}$ which affect the TRC via the normalized Gaussian bumps as in (4) with the width of each of the bump being $\sigma = 2.5$ tones. It was also assumed that the TRC measurements at $\texttt{tone}_5$, $\texttt{tone}_{17}$ and $\texttt{tone}_{30}$ were available for feedback control.

Using performance and robustness weightings of $\mathbf{W}_e = \mathbf{I}$ and $\mathbf{W}_u = 0.1\mathbf{I}$, an optimal controller D.C. gain $\mathbf{K}_{opt}$ that optimizes (5) was designed. The closed loop system matrix in (9) was chosen to be $\mathbf{A}_c = \mathrm{diag}(0.8, 0.8, 0.8)$, and the controller coefficients $\mathbf{A}$ and $\mathbf{B}$ in (6) were subsequently obtained by solving Eqs.(9) and (8). To simulate the effect of the disturbances, the desired nominal TRC was artificially shifted so that

$$\Phi_d(\texttt{tone}) \leftarrow \Phi_d^{orig}(\texttt{tone}) - 0.02 \cdot \texttt{tone}.$$

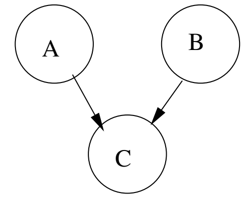

Figure 4: *A simple 3 node BBN*

where Φ_d^{orig} was the TRC when the nominal actuator settings were used. As shown in Fig. 3, the TRC converged quite closely to the shifted desired TRC.

3. Bayesian Belief Network (BBN) Model for the xerographic printer

3.1. Introduction to Bayesian Belief Network (BBN)

A process, such as xerography, can be described using a set of system variables, such as PR charged voltage, scorotron grid voltage, toner density etc. Joint probabilities of these variables describe the interrelationships between them. A Bayesian Belief Network (BBN) is a compact representation of the joint probability distribution of the various system variables [1]. Formally, a BBN is an acyclic directed graph (DAG) with nodes connected by arcs. The nodes are random variables whose values represent the observed or unobserved system variables. The arcs represent the causal relationships between variables and are quantified by the conditional probabilities that a child node attains a certain value given values of all its parent nodes. The diagnostic inference process is to determine the combination of various system variables that can generate the observed values of some of the nodes. It is performed by the application of Bayes rule in probability theory.

Because each conditional probability function that the BBN remembers generally involves only a small subset of the variables in the network, a BBN significantly reduces the storage required for the joint probability distribution, and the computational burden associated with the inference process.

A simple 3 node BBN is shown in Fig. 4. Suppose that each node can take on values of yes or no. It says that the value of node C depends on the outcomes of nodes A and B according to a joint probability table: $P(C|A, B)$ which has 8 entries. To specify the BBN in figure 4 completely, one must specify $P(C|A, B)$ as well as the prior probabilities of the ancester nodes, $P(A)$ and $P(B)$.

For example, let $P(C = \texttt{yes}|A = \texttt{yes}, B = \texttt{yes}) = 0.95$, $P(C = \texttt{yes}|A = \texttt{yes}, B = \texttt{no}) = 0.85$, $P(C = \texttt{yes}|A = \texttt{no}, B = \texttt{yes}) = 0.90$, $P(C = \texttt{yes}|A = \texttt{no}, B = \texttt{no}) = 0.02$. The entries for $P(C = \texttt{no}|A, B)$ can be computed from $P(C = \texttt{no}|A, B) = 1 - P(C =$

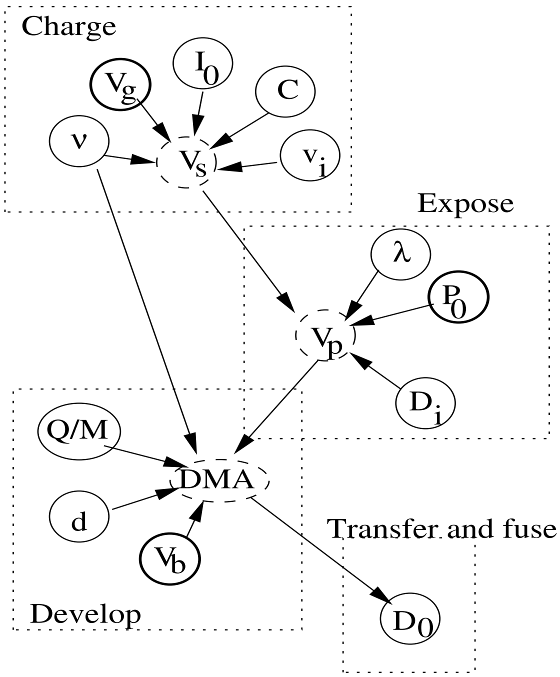

Figure 5: *A BBN for a single solid color xerographic printing process. Thick nodes are actuated variables, dashed nodes are observed variables.*

$\texttt{yes}|A,B)$. Let also $P(A = \texttt{yes}) = 0.1$ and $P(B = \texttt{yes}) = 0.1$. Suppose that we observe the evidence that $C = \texttt{yes}$. The diagnostic problem is to estimate the values of A and B. Using Bayes rule in probability, we find that $P(A = \texttt{yes}|C = \texttt{yes}) = 0.47$, $P(B = \texttt{yes}|C = \texttt{yes}) = 0.49$, and $P(A = \texttt{yes}, B = \texttt{yes}|C = \texttt{yes}) = 0.052$. From these, we can conclude that while it is reasonable to infer that $A = \texttt{yes}$ or $B = \texttt{yes}$, it is unlikely that both $A = \texttt{yes}$ *and* $B = \texttt{yes}$.

3.2. Continuous BBN for a Xerographic Printer

A simple BBN that describes the single solid color xerographic printing process is shown in Fig. 5. Notice that the BBN reflects how the processes of charge, expose and develop interact with each other sequentially. V_s and V_p denote the voltages of the photoreceptor after charging, and exposure respectively, "DMA" denote the toner mass area density after the development process, and D_0 denotes the density of the printed image on the final medium. D_i is the density of the desired image to be printed.

To complete the description of Fig. 5, we must specify the the probabilities of a child node conditional on its parents. In our model, these are obtained from physical models given in the literature. To illustrate, the ideal physical model for the charging subsystem is given by [4]:

$$\begin{aligned} V_s &= f(V_i, V_g, I_0, C, \nu) \\ &:= V_g\left(1 - e^{-\frac{I_0}{V_g}C\nu}\right) + V_i e^{-\frac{I_0}{V_g}C\nu} \end{aligned} \qquad (10)$$

where V_g is the scorotron grid voltage, V_s is the exit voltage on the photoreceptor (PR), I_0 is a scorotron response parameter, C is PR capacitance, and ν is the PR's speed. In Eq.(10), V_g is the actuator (manipulated variable), and the rest of the parameters are liable of being in faulty and degraded states.

Notice that Eq.(10) is a mathematical idealization. To model the uncertainty in the actual relationships, we define the conditional probability:

$$P(V_s|V_i, V_g, I_0, C, \nu) = N[f(V_i, V_g, I_0, C, \nu), \sigma_s] \quad (11)$$

where $N(m, \sigma)$ denotes a Gaussian distribution with mean m and standard deviaton σ. Thus, the ideal mathematical description of the process in Eq.(10) specifies the mean and σ_s specifies the reliability of this description. For our model, σ_s is guessed to be 1% of the feasible range of V_s. These are chosen for convenience only. If experimental or field data is available, distributions other than Gaussian distribution, or other values of σ_s can be used in Eq.(11).

Conditional probabilities for the exposure and the development processes are also specified similarly. BBN models for color printing systems can be composed by combining four copies (one for each of CMYK) of the BBN in Fig. 5, and using a color subtraction model to describe the combination of the primary colors to form the final color.

3.3. Discretization of BBN

The BBN model described in Section 4 is a continuous BBN since the node variables can take on values in a continuum. Currently, our ability to implement continuous BBNs is severely limited: conditional distributions can only be linear functions of the parent nodes. For continuous BBNs with arbitrary nonlinear conditional probability distributions, the BBNs must first be approximated by a discrete BBN. A discrete BBN is one in which each node can only take on finite number of values (states). The discretization process amounts to partitioning the continuous probability distribution function into intervals.

The propagation and updating of BBN is a NP-hard problem. The computational burden increases exponentially with the number of possible states at each node. The amount of memory for storing tables of conditional probabilities also increases dramatically. It is therefore, imperative that when the continuous BBN is discretized, the number of states at each node is kept at a minimum. To maximize the usefulness of discrete states, a maximum entropy criterion [3] is adopted in the determination of the optimal partition of the range of each continuous variable.

Suppose that the continuous range of the variable associated with a node has been partitioned into n segments, $a_1, a_2, \ldots a_n$. Let the prior probability of the occurrence of the i-th segment a_i be p_i. We can view the discretized node as a information source with entropy given by:

$$H(S) = -\sum_{i=1}^{n} p_i \text{Log}(p_i) \tag{12}$$

In our method, partitions are defined so that H(S) is optimized. It is easy to see that the optimal solution is such that each interval is as likely to happen as the other: $p_1 = p_2 = \ldots = p_n$. The optimization of $H(S)$ ensures that each outcome of the discrete value of the variable provides as much information as the next.

Notice that to discretize a continuous node "A" optimally, the prior probability $P(A)$ is needed. This is a computationally intensive task. For example, to discretize the V_s node in Fig. 5, one must first have obtained the $P(V_g)$ using marginization

$$P(V_g) = \sum_{V_i, V_g, \nu, C, I_0} P(V_g, V_i, V_g, \nu, C, I_0) \tag{13}$$

or similar procedures (e.g. using Bayes rule). In generally, the joint probability used in Eq.(13) must be computed recursively. We have developed an offline recursive algorithm in MATLAB (Mathworks, MA) that traverses the BBN and discretizes each node using techniques of divide-and-conquer and marginalization (see [6] for details).

3.4. Implementation on HUGIN System

HUGIN is a commercial software for implementing BBNs. Once a discrete BBN has been specified in HUGIN, one can introduce evidence into the software and the HUGIN will respond with the diagnosis. The discretized BBN for the single solid color xerographic process has been implemented on HUGIN. In fact, the discretization algorithm described above generates a file that can be read by HUGIN.

As an example, the BBN can be used in a predictive mode in which we assign various desired image density D_i in Fig. 5 to observe the output density. A probabilistic TRC can be generated this way. The near linear shape of the mode of the TRC in Fig. 6 illustrates that the BBN model is reasonable. In the diagnostic mode, one can use the observed variables to estimate the states of the unobserved variables, with which the printer's capability can be obtained. These in turn will inform how, the control strategy should be reconfigured to make the best use of the printer's current (degraded) capability.

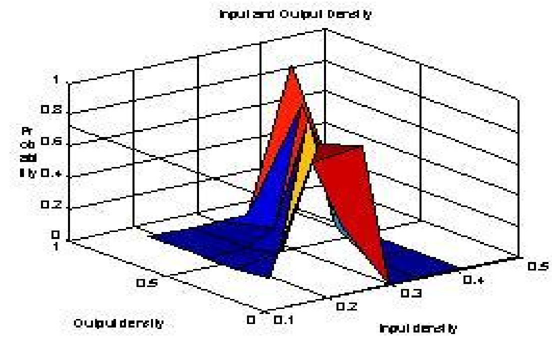

Figure 6: *The probabilistic Tone Reproduction Curve. Probability of theoutput density given input density*

4. Conclusions

We have outlined two strategies for the management of the xerographic printing process in the presence of moderate disturbances or system faults and component degradations. In the first strategy, robust control concept is applied to the stabilization of the tone reproduction curve (TRC). The key feature of this problem is that only a small number actuators and samples of the TRC are available for feedback control. The second strategy involves diagnosing the fault conditions and the degree of degradation of the system. For this purpose, a discetize Bayesian Belief Network model has been developed based on the physical models. Although we have focused on single primary color printing, similar ideas should also apply to color printing requiring combinations of primary colors.

References

[1] F. V. Jensen. *An Introduction to Bayesian Networks*. Springer-Verlag, New York, NY USA, 1996.

[2] P. Y. Li and S. A. Dianat. Robust stabilization of tone reproduction curves for xerographic processes. In *Proc. of the 1998 IEEE Conf. on Control App.*, 1998.

[3] S. Roman. *Introduction to Coding and Information Theory*. Springer-Verlag, 1991.

[4] L. B. Schein. *Electrophotography and development physics*. Springer, Berlin, 1988.

[5] R. Smith and A. K. Packard. Optimal control of perturbed linear static systems. *IEEE transactions on Automatic Control*, 41(4):579–584, 1996.

[6] C. Zhong and P. Y. Li. Bayesian belief network modeling and diagnosis of xerographic systems. In *Proceedings of the ASME Symposium on Controls and Imaging - IMECE Nov.*, 2000.